JOURNAL OF CATALYSIS 113, 475–489 (1988)

Catalytic Etching of Platinum Alloy Gauzes

DENNIS R. ANDERSON

Engelhard Research and Development Center, Edison, New Jersey 08818

Received July 22, 1987; revised March 29, 1988

Cyclic voltammetry has been used to determine catalyst gauze surface area and other related features characteristic of catalytic etching of platinum alloy gauzes used in ammonia oxidation or hydrogen cyanide production. Up until this point, surface areas of individual catalyst gauzes could not be accurately measured. The results show that the surface area of the top gauze in a catalyst pack is about 250 cm^2/g compared to the bottom layer of the pack, which is about 35 cm^2/g. Rhodium enrichment at the gauze surface is shown to be greater than 60%. Rhodium oxide can account for as much as 50% of the gauze surface area in normal catalysts and more than 90% in catalysts deactivated by rhodium oxide needle formation. It is proposed that the surface area of used gauzes is proportional to the reaction rate of ammonia and oxygen at the surface of the individual layer. The rate of growth in gauze surface area does not fit the current models available. However, the growth appears to be proportional to the logarithm of time.

INTRODUCTION

The oxidation of ammonia to nitrogen oxides for production of nitric acid and the reaction of ammonia with methane for production of hydrogen cyanide via the Andrussow process are conducted over platinum-based alloy catalyst gauzes. These gauzes experience a wide range of operating conditions. The conditions for ammonia oxidation vary from 1 to 10 atm, from 800 to 950°C for the bulk gas temperature, and from 10 to 12% ammonia inlet concentrations (*1*). The Andrussow process uses a pressure of 2 atm, a bulk gas temperature of 1100 to 1200°C, and inlet concentrations of 10 to 15%, for both ammonia and methane (*2, 3*). Under these conditions, platinum alloy gauzes quickly undergo extensive surface restructuring. The wire diameter will effectively increase by 50%, and the surface will roughen with numerous facets and pits. In addition to this restructuring, platinum, in the form of platinum oxide, is lost from the surface. Such losses are considerable in high-pressure ammonia oxidation plants, but decrease accordingly in lower-pressure plants. Due to the net reducing environment in hydrogen cyanide plants, platinum losses are negligible.

Gauze restructuring and platinum loss have been examined by a number of investigations (*3–12*). McCabe *et al.* (*4*) have explored effects of varying gas composition and sample temperature on the type of restructuring which occurs on platinum wires. They report that etching of the surface occurs much more rapidly in the presence of both oxygen and ammonia than it does in the presence of either gas alone. Thus, they postulate that the surface reaction forms an activated platinum species which is mobile. This movement is due to either the gas-phase diffusion of platinum oxide or the diffusion of platinum atoms along the surface.

Flytzani-Stephanopoulos and Schmidt (*13*) have developed a mathematical model to predict evaporation and deposition rates of platinum from a wire. Mullins (*14, 15*) also has developed a model to predict the rate of facet growth for either gas-phase or surface transport.

To date, nothing has been published in the way of quantifying the structural changes which occur on these platinum sur-

0021-9517/88 $3.00

faces. This paper describes a cyclic voltammetric method for accurately measuring surface areas of platinum-containing gauzes.

Cyclic voltammetry has been used to study platinum electrodes and to determine their surface areas by hydrogen adsorption. This method of surface area measurement is based on the fact that hydrogen can be adsorbed and desorbed from a platinum surface in an acidic solution at electrode potentials between −0.19 and 0.20 V versus a saturated calomel electrode (SCE). The equation which describes this adsorption/desorption phenomenon is

$$Pt + H^+ + e^- \leftrightarrow Pt\text{-}H \qquad (1)$$

During a cathodic potential sweep, hydrogen ions in solution are adsorbed on the platinum surface as hydrogen atoms with an electron being transferred. The process is reversed for an anodic sweep. This current can be accurately measured with a coulometer. It has been shown that the amount of charge passed is directly proportional to the surface area of the electrode. The accepted factor for both polycrystalline platinum and rhodium is 210 $\mu C/cm^2$

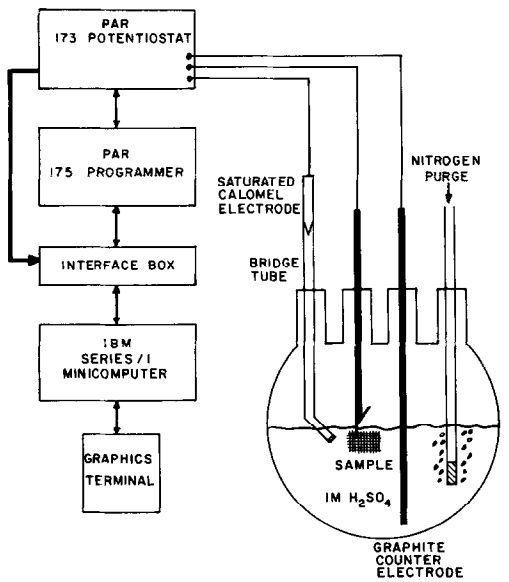

FIG. 1. Diagram of cyclic voltammetric apparatus.

(*16*). With this sensitivity, the surface area of a single wire can be measured, which is far greater than that obtainable with conventional BET instruments.

In the following section, inherent advantages and disadvantages of this technique are discussed in view of the characterization of platinum alloy gauzes. Data are presented for ammonia oxidation gauzes run under low-, medium-, and high-pressure conditions. Other data detailing surface areas of gauzes, as a function of time on-stream and position within a gauze pack, consisting of 4–25 randomly oriented gauze layers, are also given. For comparison, a hydrogen cyanide gauze is also examined.

EXPERIMENTAL

Determination of Gauze Surface Areas

A Princeton Applied Research (PAR) Model 173 potentiostat with a Model 376 logarithmic current converter and a PAR Model 175 programmer are interfaced to an IBM Series 1 minicomputer. See Fig. 1 for a schematic diagram of the apparatus. Approximately 1 cm^2 of catalyst gauze, which is two orders of magnitude less than that needed for normal BET surface area measurements, is used in the surface area measurement. Gauze surface areas are measured in the as-received condition and after a reduction step consisting of 3% H_2 in N_2 at 400°C for 30 min. This is sufficient to reduce any metal oxides in the sample without substantially restructuring the surface. The weight of the gauze, typically 40–100 mg, is recorded.

Several strands are partially separated from the sample and held by an alligator clip for electrical connection. Next, the gauze is placed into a 1 *M* sulfuric acid solution, made with deionized water and Corco reagent-grade sulfuric acid. The acid solution is deoxygenated by bubbling with nitrogen. To ensure that chloride ions do not leak into the sample compartment from the saturated calomel reference electrode, the solution is changed regularly.

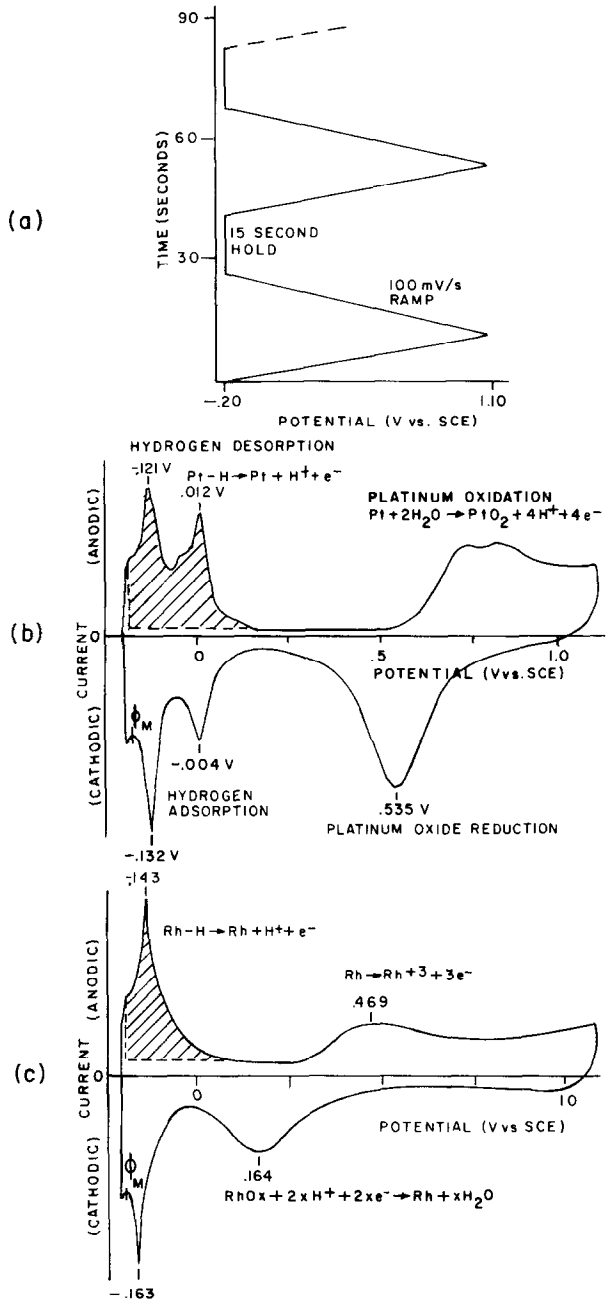

FIG. 2. (a) Representation of potential waveform used; (b) voltammogram of platinum wire; (c) voltammogram of rhodium wire.

A potential of −0.20 V versus the SCE is applied to the gauze. The potential is then varied between −0.20 V and 1.10 V at a rate of 100 mV/s in the waveform shown in Fig. 2a. The current produced as a result of the varying potential is recorded as a function of the potential. Sample voltammograms of platinum and rhodium are shown in Figs. 2b and 2c, respectively, with the regions of interest noted and annotated.

The surface area is obtained by measuring the charge associated with the hydrogen desorption peak (shaded area). All of the surface areas reported in this paper were measured after the 31st cycle.

At this point, it is useful to briefly describe the intricacies of cyclic voltammetry relevant to platinum and rhodium. First, this technique only measures contributions from metallic species in the first atomic layer which are in electrical contact with the sample holder. In the as-received samples, this phenomenon excludes any contributions from islands of rhodium oxide present on the surface. However, after the reduction step, these areas become accessible. Second, some dissolution of the metal species on the surface takes place. During potential cycling, the equivalent of two to three monolayers of rhodium are removed from the gauze. In fact, rhodium dissolution is approximately 10 times faster than platinum dissolution (*17*). Third, the surface undergoes some restructuring during the potential cycling (*18*). This should be kept in mind when making interpretations on an absolute scale. Fourth, because the peaks in the voltammograms of platinum and rhodium overlap and make the establishment of a baseline difficult, the surface area measurements were based on the hydrogen desorption peaks, contrary to the use of the hydrogen adsorption peak in the literature (*16, 18–20*). This was found to be acceptable, since the adsorption and desorption peak areas are essentially equal for platinum and rhodium alone. Finally, the degree of coverage of hydrogen on platinum and rhodium is between 80 and 90% of a monolayer (*16*). None of the data reported in this paper have been adjusted for this effect. The surface area of a virgin piece of gauze is determined to be 26 cm^2/g with an accuracy of approximately $\pm 10\%$. This compares to a value of 25 cm^2/g based on the geometric area. A roughness factor of 1.25 is expected on these wires and would be accounted for with a full monolayer coverage.

Catalyst Gauze History

Four commercial catalyst gauzes were characterized and are designated A–D. Their operating pressures varied from 1.5 to 8 atm and their time on-stream varied from 3 months to 1 year. All other gauzes were run in Engelhard's laboratory pilot plant. This pilot plant is capable of operating between 4 and 9 atm at flow rates of up to 7.90 liters/s (1000 SCFH). The ammonia concentration is variable over the range 5–15%. The air is preheated to 200–300°C prior to entering the combustion chamber. The gauze samples are 3.18 cm (1.25 in.) in diameter with the exposed area being 2.54 cm (1 in.) in diameter. The gas exit temperature is monitored by a thermocouple placed 2.54 cm (1 in.) below the gauze pack. The NO_x yield varied between 89 and 99% depending upon the operating parameters.

The gauze alloy compositions were either 90/10 (weight percent) Pt/Rh or 90/5/5 Pt/Rh/Pd. No attempt was made to distinguish between the two alloys. Samples from the gauze packs were separated into individual layers. During this separation process, some particulate matter was lost from the gauzes, which was a problem with some samples from commercial plants. However, the particulates tend to be rich in nonprecious metals and therefore do not significantly impact the surface area measurements. Electron micrographs were taken with an ISI DS130 scanning electron microscope (SEM).

RESULTS

A number of different aspects of the surface of these gauzes can be studied by cyclic voltammetry and each will be considered in turn. These include enrichment of rhodium on the gauze surface, presence of rhodium oxide on the surface, changes in gauze surface area with position and time on-stream, effects of reactor pressure and throughput, crystallographic orientation of platinum, and a comparison of HCN and AMOX gauzes.

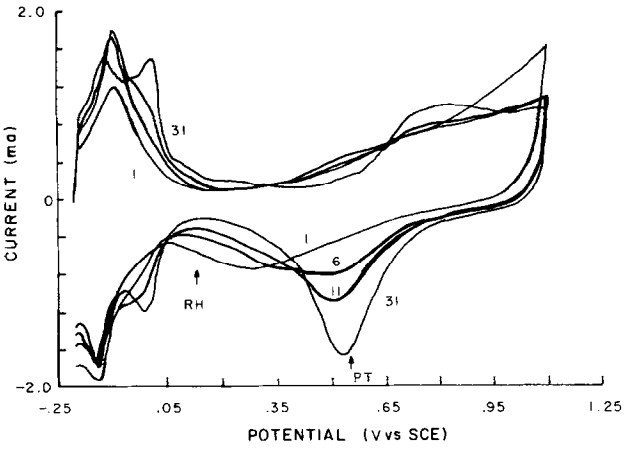

FIG. 3. Cyclic voltammograms of a platinum/rhodium gauze after 1st, 6th, 11th, and 31st cycles. Positions of the oxide reduction peaks for platinum and rhodium are noted.

All surface area data are reported in units of square centimeters per gram, based on the weight of a new gauze, thereby putting all gauzes on the basis of measured surface area per unit frontal area of gauze. Except where noted, all surface area data and voltammograms are from reduced gauzes.

Rhodium Enrichment

By following the pattern of the cyclic voltammograms from the 1st to the 31st cycle, several observations can be made for an unreduced gauze. These can be seen in Fig. 3. The first cycle is indicative of a high-rhodium-content alloy. For pure rhodium, the rhodium oxide reduction peak occurs at 0.16 V versus the SCE; for platinum, the oxide reduction peak occurs at 0.53 V versus the SCE. The position of the minimum corresponding to the oxide reduction peak on the first cycle is 0.27 V. A linear interpolation between the pure oxide reduction peaks shows a rhodium content on the surface of 70% for this sample, considerably higher than the bulk concentration of the alloy. The rhodium concentration at the surface varies from about 60% to as much as 100% on a metal basis for severely deactivated samples. As the gauze potential is cycled, the rhodium layer is dissolved into solution revealing more platinum in the subsequent atomic layers. Contributions from at least two peaks can be seen in cycle 6. This is because some areas of the gauze have higher rhodium contents than others. Depending upon the amount of rhodium enrichment in the gauze surface, the final scan will resemble that of platinum with contributions from any patches of rhodium-rich alloys that may have accumulated on the surface. Baker *et al.* (*17*) have observed similar results in their studies of platinum–rhodium alloys.

Gauze Surface Area by Layer

The surface areas of a number of gauze sets are shown in Fig. 4. It can be seen that

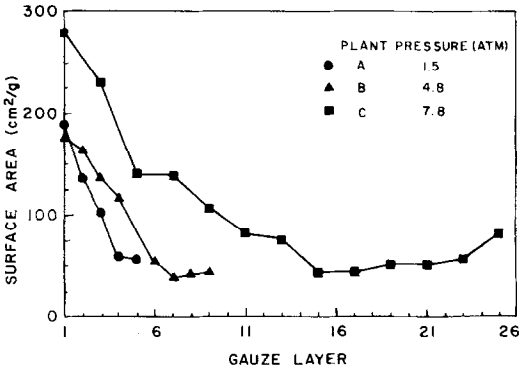

FIG. 4. Gauze surface area versus position within the pack for three ammonia oxidation plants.

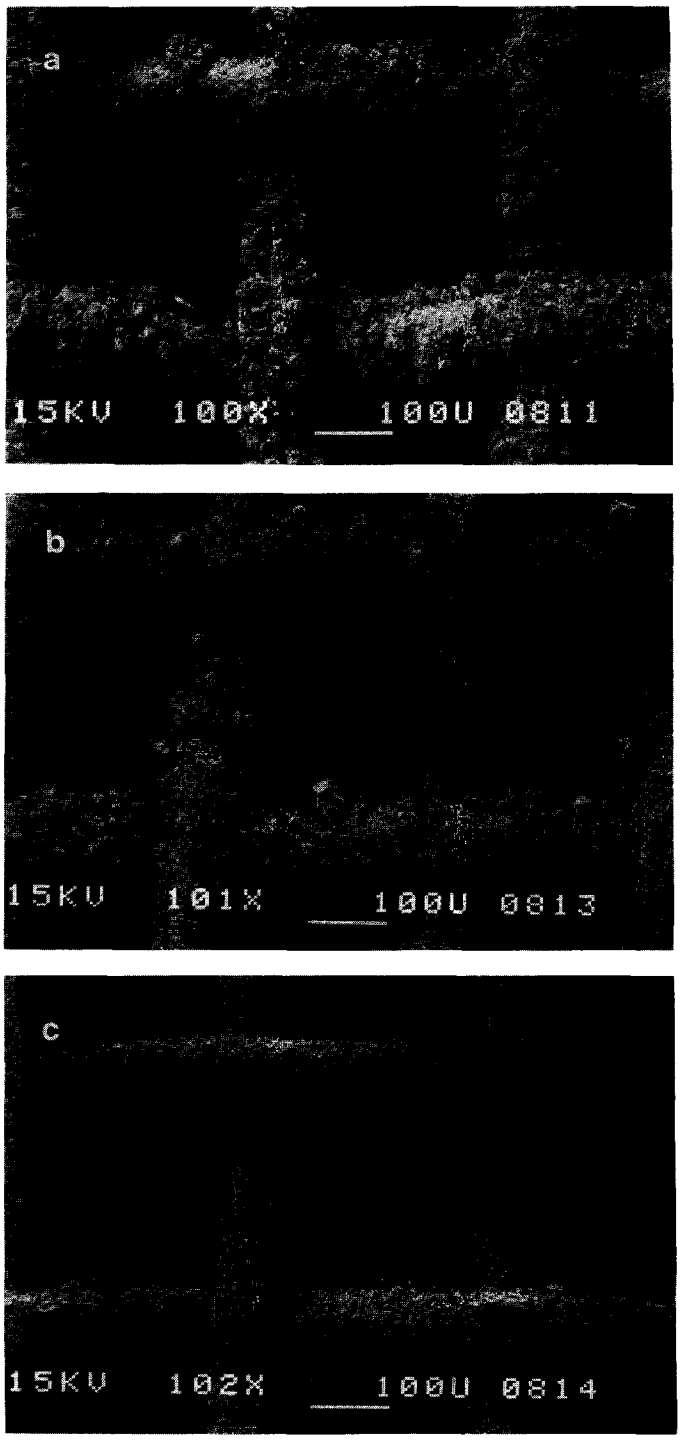

FIG. 5. Electron micrographs of Plant "C" gauze: (a) 1st layer, 100×; (b) same, 1000×; (c) 5th layer, 100×; (d) same, 1000×; (e) 10th layer, 100×; (f) same, 1000×.

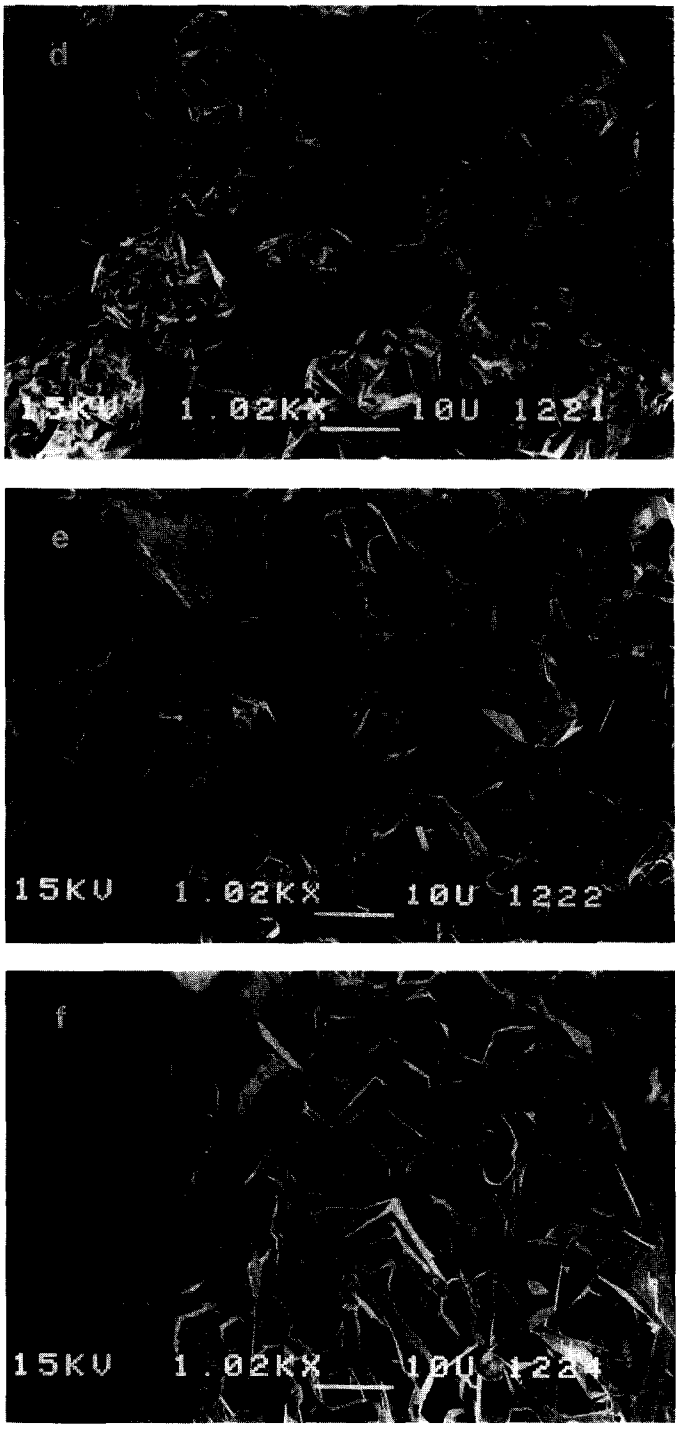

FIG. 5—*Continued.*

the top gauze in the gauze pack has the highest surface area. Its surface area has increased by an order of magnitude from that of a fresh gauze. The surface area decreases through the gauze pack with the lower layers showing only a moderate increase in surface area. There is a modest upturn at the bottom of the pack due to the presence of a small number of rhodium oxide needles.

The micrographs shown in Fig. 5 illustrate the change in the surface morphology as a function of layer. In the first layer, the surface of the gauze has numerous growths protruding from the wire surface. As a result, the effective wire diameter has almost doubled. Photographs of the 5th and 10th layers show smaller and fewer growths which would be in agreement with a lower surface area. The facetting of the surface is also less noticeable on the lower layers.

There are several areas where growths appear to be missing. These are places where the adjacent gauze layers were touching or where growths had been attrited during use or separation of individual gauzes from the gauze pack.

Pressure Effects on Surface Area

Figure 4 also compares surface areas obtained for a gauze from a typical high-pressure plant (8 atm), a medium-pressure plant (5 atm), and a low-pressure plant (1 atm). It can readily be seen that surface area drops off much more rapidly in low-pressure gauzes than in higher-pressure gauzes. This is because the percentage conversion is higher on the initial layers of a low-pressure gauze than that for a high-pressure gauze.

Rhodium Oxide Contributions

With the surface of the gauze being covered to a large extent by rhodium and rhodium oxide, it is not surprising that islands of rhodium oxide would complicate the interpretation of the results. Rhodium oxide is nonconducting. Thus, portions of the surface are electrically isolated and do not contribute to the total surface area. This can be seen most readily in samples covered with a thick layer of rhodium oxide. If the surface area of a gauze is measured after the reduction step, it may increase by a factor of 2 to 3 times that of the unreduced surface area. By examining the ratio of these two surface areas, it may be possible to determine the degree of gauze deactivation by rhodium oxide formation. SEM examination of surface morphology shows that surface structures do not change as a result of the reduction step. Therefore, it can be expected that surface area results are indicative of the rhodium oxide content.

Rhodium oxide needles form as a result of operating at a low temperature and high oxygen partial pressures. These needles tend to form preferentially on the lower layers and can yield surface areas of 1000 cm^2/g or more after they have been reduced.

Figure 6 illustrates how rhodium oxide on the surface affects surface area. The lower curve corresponds to the as-received gauze. Once the sample is reduced, the surface area increases as shown in the upper curve. If rhodium oxide needles have not formed, the topmost layers experience the largest percentage increase in area.

Surface Area Changes with Time

Figure 7 illustrates the changes which occur in surface area of a gauze as a function of time on-stream. The surface area of the first layer changes quite rapidly during the first hour of pilot plant operation, increasing by a factor of 3 within the first 15 min alone. At the end of 20 h, the surface area has increased to about 70% of its final value. On subsequent layers, the rate of increase is lower. Within 1 week the surface is almost fully sprouted. This agrees with the experience of plant operators. Gauzes in commercial plants are expected to be fully activated in 4 to 5 days.

The photographs in Fig. 8 show the change in surface morphology with time. Figure 8b depicts the down-stream side of the top layer after 15 min of operation.

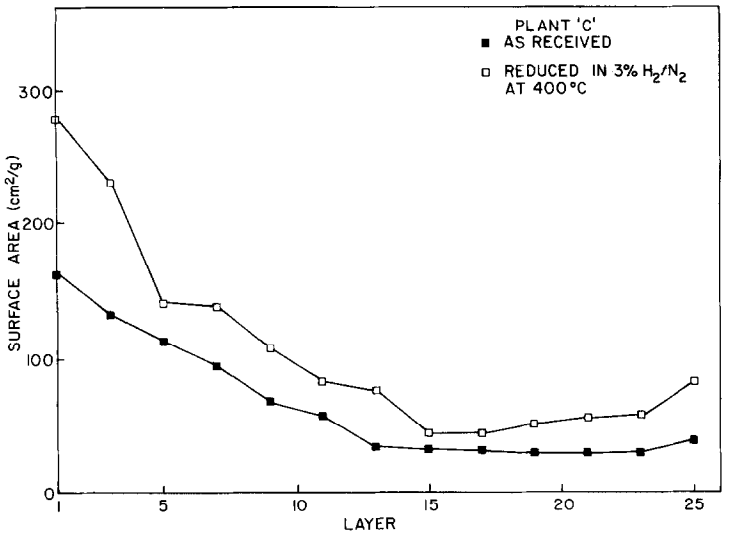

FIG. 6. A comparison of surface areas obtained for reduced and unreduced Plant "C" gauzes.

Since the boundary layer between the gauze surface and the gas stream is smallest at the front face of the gauze and increases toward the back face, the edge of the gauze shows the greatest amount of etching in this micrograph. Regions near the intersection of the wires, and at the center of the wire surface where the boundary layer is thickest, show the least amount of etching. As the time on-stream increases, the number of growths decreases with a corresponding increase in their size.

Crystallographic Orientation of Platinum

The voltammograms of platinum single crystals have been studied by Will (*18*) and more recently by Ross (*20*). They show that each crystalline face has a unique cyclic voltammetry pattern. The (111) and (110) crystal faces contribute strongly to the

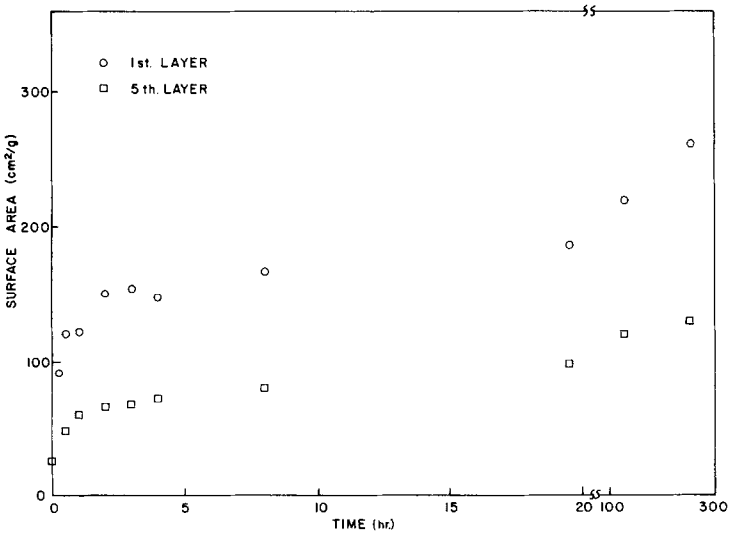

FIG. 7. Surface area of first and fifth layers versus time on-stream.

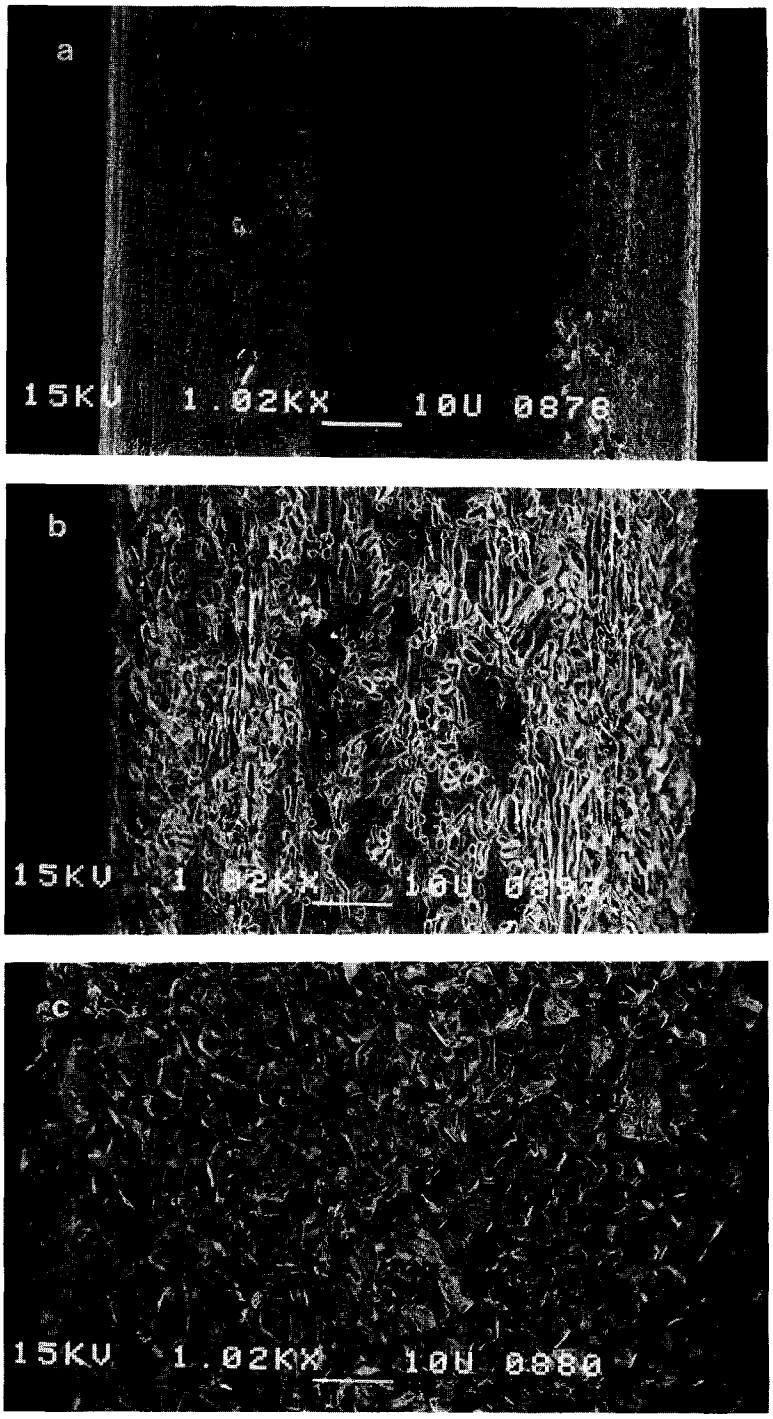

FIG. 8. Electron micrographs of top layer versus time on-stream: (a) new; (b) 15 min; (c) 30 min; (d) 1 h; (e) 4 h; (f) 19.5 h. All photographs at 1000×.

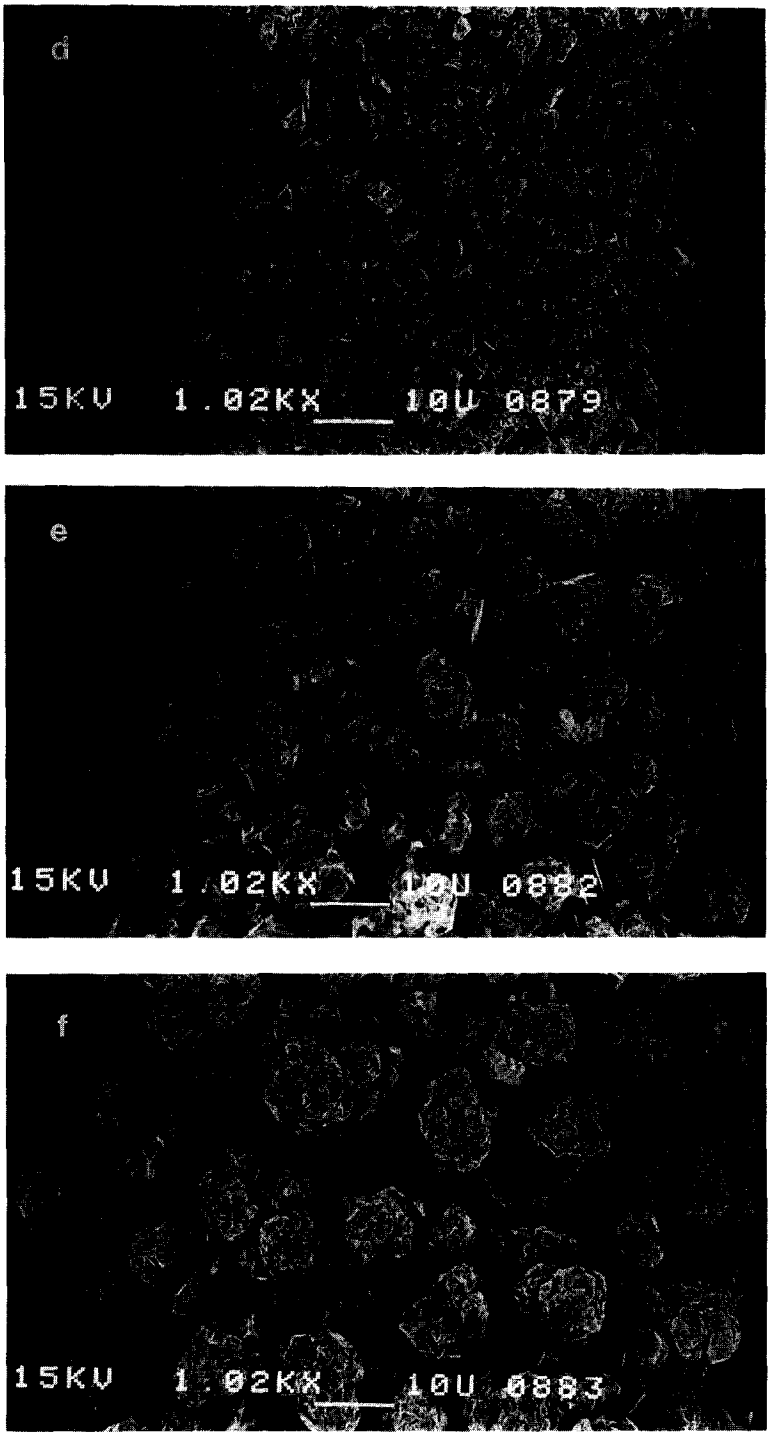

FIG. 8—*Continued.*

lower potential peak at −0.121 V, while the (100) face contributes to the higher potential peak at 0.012 V.

Differences have been seen in the relative intensities of the two hydrogen desorption peaks as a function of time on-stream and position within the catalyst bed. However, since rhodium dissolution and platinum surface restructuring occur during potential cycling, no definitive conclusions can be made.

HCN Gauze versus Ammonia Oxidation Gauzes

Due to the brittleness and the tendency of the gauze layers to fuse together, individual layers of the HCN gauze could not be separated. The top five layers were measured as one piece, and the surface area was determined to be 114 cm^2/g. This agrees well with the value obtained by Pan (*8*) by gas adsorption techniques, but the basis for comparison is uncertain, since he may have measured the entire pack or may have had a different gauze geometry. No direct comparison can be made between the HCN gauze and the ammonia oxidation gauzes because of the vast differences in the operating conditions, but the surface area is similar to that expected for ammonia oxidation gauzes.

Examination of the voltammograms for rhodium enrichment reveals an entirely different result than that seen for ammonia oxidation gauzes. The oxide reduction peak on the first cycle consists of two peaks at 0.31 and 0.49 V, which correspond to alloy compositions of 60 and 10% rhodium, respectively; the 10% peak is the major. This is expected since HCN gauzes experience a net reducing atmosphere, and as a result the amount of rhodium oxide formation and platinum oxide volatilization is minimal.

DISCUSSION

Surface Area Variation with Position

In the plot of surface area versus gauze layer, the surface area decreases monotonically in much the same manner as the ammonia concentration would be expected to decrease. Therefore, the reaction profiles were calculated for each gauze set based on a method presented by Satterfield and Cortez (*21*) and Shah and Roberts (*22*). The following equations were used to determine the relative yield per layer for a mass transfer controlled reaction. The Reynolds number is calculated by

$$N_{\mathrm{Re}} = \frac{d \cdot G_0}{\delta \cdot \mu}, \tag{1}$$

where d is the wire diameter, G_0 is the superficial velocity of the reactants, μ is the viscosity, and δ is the fractional open area and is defined by

$$\delta = (1 - N \cdot d)^2, \tag{2}$$

where N is the wire mesh density. In all cases, the starting wire diameter was used in the calculations and was assumed to remain constant. The Reynolds number was used to calculate the j factor, according to the relationship determined by Shah and Roberts,

$$j_{\mathrm{D}} = 0.644 N_{\mathrm{Re}}^{-0.57}. \tag{3}$$

The j factor is also related to the percentage conversion by the equation

$$j_{\mathrm{D}} = (N_{\mathrm{Sc}}^{2/3}/A_{\mathrm{T}}) \ln(C_{\mathrm{i}}/C_{\mathrm{o}}), \tag{4}$$

where N_{Sc} is the Schmidt number, A_{T} is the surface area of the gauze per square centimeter of frontal area, and C_{i} and C_{o} are the inlet and outlet concentrations of the limiting reagent, respectively. A value of 0.81 was used for the Schmidt number (*21*). A surface area of 1.56 cm^2 used in the calculations was based on the initial wire diameter and wire mesh. This approximates the mass transfer area across the boundary layer and provides better results than if the real surface area was used. All of the other parameters were estimated from the nominal operating parameters of the plants.

The fractional conversion of the feed stream per layer, dY_1, is given by

$$dY_1 = 1 - \frac{C_o}{C_i}. \quad (5)$$

The conversion on the subsequent n layers can be determined by

$$dY_n = \left(1 - \sum_{i=1}^{n-1} dY_i\right) \cdot dY_1, \quad (6)$$

where the first term represents the fraction of ammonia unreacted before the nth layer. The mass transfer controlled reaction rate is given by

$$R_n = \frac{k_m \cdot r \cdot x_n}{M} = \frac{dY_n \cdot G_0 \cdot C_a}{M} \quad (\text{mol/cm}^2/\text{s}), \quad (7)$$

where k_m is the mass transfer coefficient, r is the gas density, x_n is the weight fraction of ammonia unreacted on the nth layer, M is the molecular weight of ammonia, G is the mass thruput of the reactor, and C_a is the initial weight fraction of ammonia in the gas stream.

In Fig. 9, surface area data are plotted versus the reaction rate for each of these gauzes. The correlation for the high-pressure plants is very good. The lower-pressure plants show some curvature. This could be due to the model predicting higher reaction rates on the leading gauzes than actually occur.

There are a number of sources for error associated with the calculation of the reaction rate. First, the real surface area, the percentage open area for each gauze layer, and the effective wire diameter are all changing as a function of the gauze position. Second, the error associated with the calculation of the j factors themselves is approximately 10%. Third, the temperature of the gas was taken to be the gas exit temperature. In the initial layers, the gas temperature will be less than that at the gauze exit, particularly in the case of high-pressure gauzes. This affects the gas viscosity as well as the density term in Eq. (7). Fourth, the flow distribution and mixing of the ammonia are also important in this calculation.

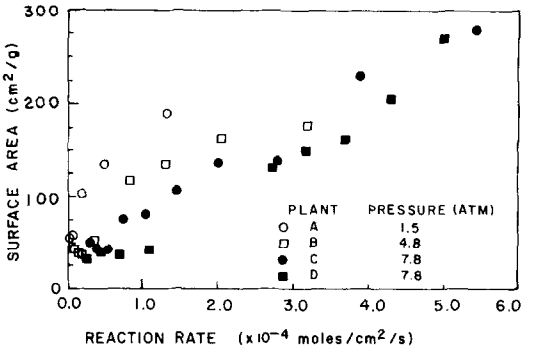

FIG. 9. Gauze surface area as a function of the calculated reaction rate.

A gauze pack with an uneven flow distribution across its face will have different Reynolds numbers at various points and, as a result, different reaction rates for the same nominal flow rate. Fifth, nominal operating conditions of the plants were used in the calculations. The actual operating conditions may not correspond to these values. With these things in mind, the correlations presented in Eq. (7) are reasonable.

Surface Area Variation with Time

Mullins (*15*) has developed a model to describe facetting which may occur by gas-phase diffusion or by surface diffusion of the metal atoms. In his model, Mullins concludes that the growth rate of the depth and width of a facet by gas-phase diffusion is proportional to the cube root of time. The rate of surface diffusion, on the other hand, is proportional to the fourth root of time.

In an analogous manner, the surface area of a facet should vary in much the same way and behave according to the equation

$$S \sim K \cdot t^m + S_0, \quad (8)$$

where S is the measured surface area, K is a derived constant according to Mullins, t is the elapsed time, m is a fractional power, and S_0 is the initial surface area. In Fig. 10, the log of the change in surface area is plotted versus the log of the elapsed time. A least-squares fit was obtained over the entire range of time on-stream. The roots for

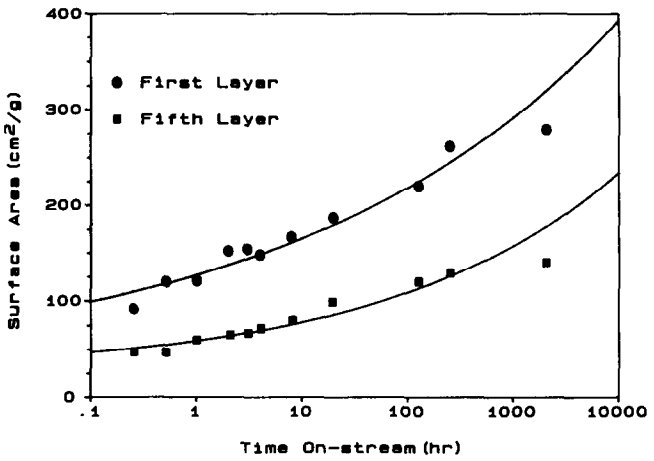

FIG. 10. A fit of surface area data to the fractional power of time.

the first and fifth layers are 0.14 and 0.20, respectively. Both roots are lower than those values predicted by Mullins. If times on stream of less than about 4 h are used, values intermediate to one-third and one-fourth are obtained. Over the time span in which these experiments were conducted, it is quite likely that the surface area is approaching a steady-state value and forcing the power dependence to an artificially low value.

This steady-state condition consists of the mechanism of facet growth being counterbalanced by the increased losses of surface area by oxide volatilization and surface sintering. Growth of a rhodium oxide barrier, loss of platinum and rhodium from the surface, effects of bulk diffusion, and development of thermodynamically stable crystal faces all contribute to establishing this steady-state condition.

From Fig. 10, it can be seen that a better fit to the data would be a simple logarithmic dependence on time, as

$$S = K \cdot \log_{10}(t) + S_0, \qquad (9)$$

where S is the surface area, K is a constant, t is the time on-stream, and S_0 is a constant. There is no model in the literature which predicts this type of behavior. The only theory which gives an analogous behavior is the Elovich isotherm (*23*).

SUMMARY

It has been shown that a number of different aspects of catalytic etching can be and have been addressed by cyclic voltammetry. They are the following.

(i) The powerful technique of cyclic voltammetry has been applied to the study of catalytic etching of platinum alloys with great success. This opens the door to many far-ranging studies concerning the use of electrochemical techniques to probe mechanisms of catalytic etching on noble metals. While the use of cyclic voltammetry to study platinum etching will be most useful and yield the best data, other noble metals, such as rhodium and iridium, are amenable to this type of study.

(ii) The surface area of a gauze is directly proportional to the reaction rate on its surface.

(iii) The rhodium concentration in the gauze surface can be measured and is typically 60–100% of the outer atomic layer for ammonia oxidation gauzes. HCN gauzes, on the other hand, show little enrichment with the majority of the surface having the same composition as the bulk.

(iv) The surface coverage of rhodium oxide can be determined and can possibly be used to estimate the degree of gauze deactivation.

(v) The change in surface area with time can be fit to either a power dependence or a logarithmic dependence on time.

Additional topics for investigation by this technique include the effects of alloy composition on surface area and orientation, the effects of different reactions and heats of reaction on the surface area, and the effects of fuel rich reactions mixtures on the catalytic etching process. A number of these studies have already been presented in the literature, except that the surface area was not determined.

ACKNOWLEDGMENTS

The author acknowledges the aid of several persons: S. Goresh for her aid in obtaining the cyclic voltammetry data, B. Nartowicz and T. Piotrowski for providing the SEM photographs, H. Lee for his aid in obtaining and producing samples, and both H. Lee and J. Hochmuth for their very helpful technical discussions.

REFERENCES

1. Sperner, F., and Holmann, W., *Platinum Met. Rev.* **20,** 12 (1976).
2. Satterfield, C. N., "Heterogeneous Catalysis in Practice." McGraw-Hill, New York, 1980.
3. Knapton, A. G., *Platinum Met. Rev.* **20,** 131 (1978).
4. McCabe, R. W., Pignet, T., and Schmidt, L. D., *J. Catal.* **32,** 114 (1974).
5. Philpott, J. E., *Platinum Met. Rev.* **15,** 52 (1971).
6. Flytzani-Stephanopoulos, M., Wong, S., and Schmidt, L. D., *J. Catal.* **49,** 51 (1977).
7. Pielaszek, J., *Platinum Met. Rev.* **28,** 109 (1984).
8. Pan, B. Y. K., *J. Catal.* **21,** 27 (1971).
9. McCabe, A. R., and Smith, G. D. W., *J. Phys. Colloq. C* **9,** 483 (1984).
10. Contour, J. P., Mouvier, G., Hoogewys, M., and Leclere, C., *J. Catal.* **48,** 217 (1977).
11. Schmidt, L. D., and Luss, D., *J. Catal.* **22,** 269 (1971).
12. Wu, N. L., and Phillips, J., *J. Phys. Chem.* **89,** 591 (1985).
13. Flytzani-Stephanopoulos, M., and Schmidt, L. D., *Chem. Eng. Sci.* **34,** 365 (1979).
14. Mullins, W. W., *J. Appl. Phys.* **28,** 333 (1957).
15. Mullins, W. W., *Philos. Mag. Ser. 8* **6,** 1313 (1961).
16. Woods, R., *J. Electroanal. Chem.* **49,** 217 (1974).
17. Baker, B. G., Rand, D. A. G., and Woods, R., *J. Electroanal. Chem.* **97,** 189 (1979).
18. Will, F. G., *J. Electrochem. Soc.* **112,** 451 (1965).
19. Bett, J., Kinoshita, K., Routsis, K., and Stonehart, P., *J. Catal.* **29,** 160 (1973).
20. Ross, P. N., Jr., *Surf. Sci.* **102,** 463 (1981).
21. Satterfield, C. N., and Cortez, D. H., *Ind. Eng. Chem. Fundam.* **9,** 613 (1970).
22. Shah, M. A., and Roberts, D., *Chem. React. Eng. II* **20,** 259 (1974).
23. Aharoni, C., and Tompkins, F. C., "Advances in Catalysis" (D. D. Eley, P. W. Selwood, and P. B. Weisz, Eds.), Vol. 21, p. 1. Academic Press, San Diego, 1970.